Acid−Base Behavior Study of Glycinamide Using Density Functional Theory

Ping Li,[†] Yuxiang Bu,*[,†,‡] Hongqi Ai,[†] and Zhaohua Cao[†,§]

Institute of Theoretical Chemistry, Shandong University, Jinan 250100, P. R. China, Department of Chemistry, Qufu Normal University, Qufu 273165, P. R. China, and Chemistry Group, Heze Medical College, Heze 274030, P. R. China

Received: November 23, 2003; In Final Form: February 17, 2004

A total of 9 and 10 representative structures have been located on the potential energy surfaces (PES) of protonated and deprotonated glycinamide, respectively, to investigate the acid−base behavior of neutral glycinamide employing the B3LYP/6-311++G** level of theory. In the protonation processes, the proton affinities (PA) and gas-phase basicities (GB) for the three active sites, that is, the carbonyl oxygen, amide nitrogen, and amino nitrogen, have been studied. The global minimum is characterized by an intramolecular H-bond formed between the carbonyl oxygen and one of the hydrogen atoms at the amino nitrogen site, which is consistent with most protonated amino acids. The favorable protonation site is the amino nitrogen atom followed by the carbonyl oxygen and the amide nitrogen atoms. The calculated PA for the global minimum of neutral glycinamide, 216.81 kcal/mol, is in good agreement with the experimental value (217.73 kcal/mol), indicating that glycinamide behaves as an amino nitrogen-base in the gas phase. For the deprotonation processes, the losses of protons at three possible sites, that is, the amide, amino, and carbolic hydrogen atoms, have been considered, respectively. Similarly, the global minimum is also characterized by an intramolecular H-bond formed between the amide nitrogen atom and one of the hydrogen atoms at the amino site, which is further confirmed by higher-level calculations, such as MP2, MP3, MP4(SDQ), and CCSD(T) levels, including full electron correlations. The relative order in the calculated PAs and GBs of the three sites for the deprotonated glycinamide is N3 > C2 > N4, indicating that glycinamide behaves as an amide nitrogen-acid in the gas phase. Additionally, temperature and solvent effects on the protonation and deprotonation processes have been discussed qualitatively.

1. Introduction

Acid−base behavior associated with protonation or deprotonation processes are fundamental properties in predicting chemical reactivity for biological systems in acid−base chemistry and biochemistry.[1,2] Calculated proton affinities (PA) and gas-phase basicities (GB) are also major thermodynamic parameters available for a quantitative understanding of the intrinsic properties in the absence of solvents. Moreover, the fragmentation patterns influenced by protonation in mass spectroscopy experimentally can be rationalized quantitatively via the knowledge of the proton attachments and their corresponding PA values.[3−5] In recent years, studies on the protonation and deprotonation processes for various systems have become popular subjects.[1−43] Experimentally, the ionized compounds can be easily obtained using various methods,[6] such as chemical ionization, fast atom bombardment ionization, electrospray ionization, or matrix-assisted laser desorption ionization. The PAs and GBs can be determined employing the most-used three methods, that is, equilibration measurements, reaction bracketing, and kinetic methods. However, there are some limitations when treating some systems that are thermally labile and nonvolatile and have intramolecular H-bonds or possess several possible sites for protonation, despite their merits.[6] For common biological systems containing more active sites, it is difficult to measure the PAs for the less active sites experimentally since experiment can only give the PAs for the most active sites.[3] Moreover, geometries or structural changes for the systems investigated are still difficult to obtain. On the other hand, theoretical calculations based on various theories and methods have proven to be a useful tool to explore protonation processes since they are capable of providing information about all possible sites of protonation within a given molecule on an equal footing.[7] What is more, the applications of theoretical calculations are important for those chemical systems that are not amenable to experiments.

Glycinamide, as a representative model compound containing the peptide bond, has been investigated in the past experimentally and theoretically.[8,44−53] For example, the formation of the peptide bond in glycinamide uncatalyzed or catalyzed by metal cations or ammonia has been extensively studied.[44−47] Klassen et al. reported the collision-induced dissociation threshold energies of protonated glycinamide determined with a modified triple-quadrupole mass spectrometer.[48] The unimolecular chemistry of protonated glycinamide and its PA determined by mass spectrometric experiments and theoretical modeling has been reported by Kinser et al.[8] The interrelationship between conformations and theoretical chemical shift has been investigated by Sulzbach et al.,[49] in which some useful conformational information has been mentioned at the restricted Hartree−Fock (RHF) theory and 6-31G* basis set. Ramek et al. discussed the basis-set influence on the nature of the conformations of glycinamide (minimum or saddle point) in ab initio self-consistent field (SCF) calculations.[50] Recently, all the possible conformers of glycinamide in the gas phase and in solution have

[†] Shandong University.
[‡] Qufu Normal University.
[§] Heze Medical College.

10.1021/jp037567x CCC: $27.50
Published on Web 04/09/2004

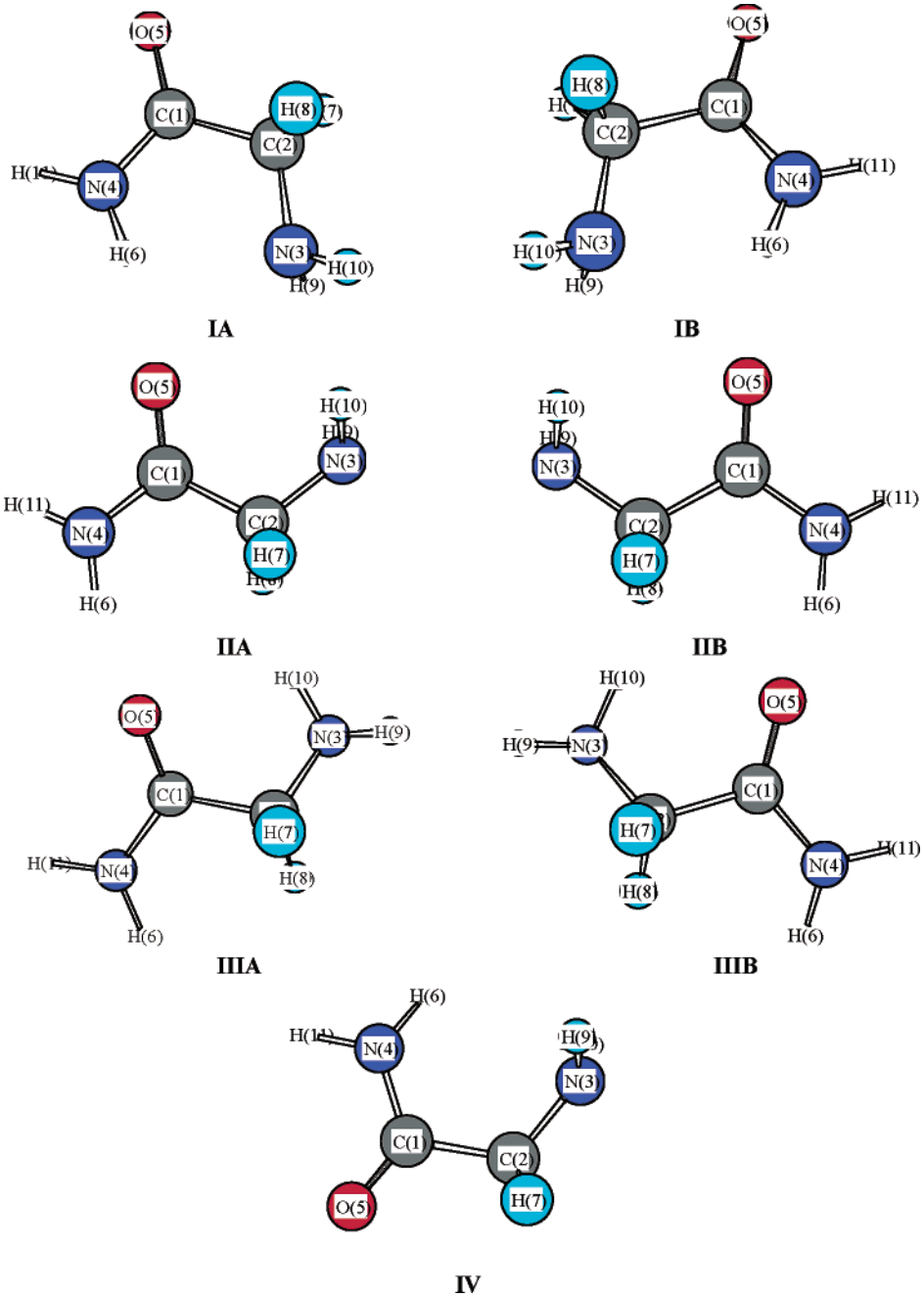

Figure 1. Optimized glycinamide conformers at the B3LYP/6-311++G** level of theory.

been systematically explored by us, in which three pairs of mirror-image conformers and one C_s symmetry conformer have been found on the global potential energy surface (PES) of glycinamide employing the B3LYP/6-311++G** level of theory.[51,52] Additionally, the ionization potentials and electron affinities of glycinamide in the gas phase and in solution have also been predicted theoretically.[53] In those studies,[51,53] the reliability of the B3LYP/6-311++G** level of theory was verified through comparisons with higher-level calculations including MP2, MP3, MP4(SDQ), and CCSD(T) levels. However, the acid−base behavior of glycinamide has not been extensively and systematically explored, except that the PAs and GBs for glycinamide have been mentioned as general information[51] and Kinser et al. have investigated PAs as described above.[8] In principle, there are three protonation sites in glycinamide, namely, N3, N4, and O5 (see Figure 1). The PAs and GBs for the three sites except for amino N3 have not been studied. Moreover, the relative stabilities among the available protonated or deprotonated glycinamide conformers and the relative orders in magnitude for PAs among the three protonation sites of glycinamide need to be further determined, where the three protonated glycinamide conformers mentioned by Kinser et al. are only a part of the nine conformers in our present studies. Unfortunately, the neutral glycinamide conformer used by Kinser et al. corresponds to the second stable conformer studied by us. For the deprotonation processes, to our best knowledge, the deprotonations at the three sites in glycinamide, namely, N4, N3, and C2 (see Figure 1), have never been reported experimentally and theoretically. Thus, it is necessary to carry out the present study to fill a void in the available data for glycinamide.

2. Computational Details

The B3LYP/6-311++G** level of theory has been used throughout the calculations, which has proven to be reliable and

TABLE 1: Relative Energies (in kcal/mol) and ZPVEs (in kcal/mol) for Protonated Glycinamide Conformers at Various Levels of Theory[a,b,c]

conformers	B3LYP	ΔZPVE	MP2	MP3	MP4(SDQ)	CCSD(T)
P1(N3)	0.0(0.0)[0.0]	0.0	0.0	0.0	0.0	0.0
P2(N4)	20.89(19.76)[25.81]	−1.13	19.20	18.87	18.21	18.35
P3(N4)	29.52(27.42)[28.44]	−2.11	28.68	29.19	27.79	27.95
P4(N4)	30.63(28.10)[31.55]	−2.53	29.62	30.07	28.68	28.91
P5(O5)	7.04(6.45)[16.12]	−0.59	7.81	4.28	6.13	6.30
P6(O5)	2.50(2.03)[11.81]	−0.48	3.20	0.80	2.34	2.13
P7(O5)	8.47(7.86)[16.97]	−0.62	9.30	5.92	7.68	7.86
P8(O5)	18.38(17.34)[22.06]	−1.04	19.97	16.34	17.87	18.26
P9(O5)	17.35(16.49)[22.59]	−0.86	18.22	14.53	16.04	16.36

[a] The total energies for P1(N3) with B3LYP, MP2, MP3, MP4(SDQ), and CCSD(T) methods are −265.0155584, −264.3873045, −264.4103949, −264.4239168, and −264.4555853 hartrees, respectively. For P1(N3), the ZPVE obtained at the B3LYP/6-311++G** level of theory is 66.50 kcal/mol. [b] The data in parentheses refer to the relative energies with ZPVE corrections. [c] The data in brackets refer to the relative energies in aqueous solution obtained employing the IPCM model within the framework of SCRF theory. The solvation energy of P1(N3) is −72.74 kcal/mol.

efficient in our recent studies.[51−53] As mentioned above, only one of the mirror-image conformers (IB, IIB, and IIIB) and the C_s symmetry conformer (IV) have been considered since the mirror-image conformers are identical to each other in energy and in structural parameters except for the dihedral angles. All the possible geometries for the protonated and deprotonated glycinamide conformers are fully optimized without any symmetry constraints on the basis of the optimized neutral glycinamide conformers available as displayed in Figure 1. Harmonic vibrational frequency calculations have been performed for optimized geometries to further confirm their stabilities and to provide thermodynamic parameters required by the calculations of PAs and GBs. None of these frequencies are scaled due to the ability of DFT calculations to predict harmonic vibrational frequencies accurately as proposed by Johnson et al.[54]

To further confirm the relative stabilities among the available conformers, single-point energy calculations have been performed employing higher-level calculations including second-, third-, and fourth-order Møller−Plesset theory (abbreviated as MP2, MP3, and MP4(SDQ)) and the coupled cluster method (CCSD(T)) including the single, double, and perturbative triple excitation. Full electrons have been considered in the above higher-level calculations.

For the following protonation process, that is, $B + H^+ \rightarrow BH^+$, the enthalpy changes and Gibbs free energy changes can be calculated as

$$\Delta H = E(BH^+) - E(B) - E(H^+) + \Delta(PV) = E(BH^+) - E(B) + E'_{vib}(BH^+) - E'_{vib}(B) - 2.5RT \quad (1)$$

$$\Delta G = \Delta H - T\Delta S \qquad (\Delta S = S(BH^+) - S(B) - S(H^+)) \quad (2)$$

where the $E(i)$, $E'_{vib}(i)$, and $S(i)$ refer to the total energy, zero-point vibrational energy (ZPVE) also including the thermal vibrational corrections to the total energy for simplicity, and entropy of the species i, respectively. As a rule, GB and PA are defined as the negative value of the Gibbs free energy changes and enthalpy changes, that is, $GB = -\Delta G$, $PA = -\Delta H$, respectively. Thus, the PA and GB are related by the entropy term: $GB = PA + T\Delta S$. Obviously, the larger the value of the PA or GB is, the stronger the base B is. For the deprotonation process, that is, $BH \rightarrow B^- + H^+$, the corresponding PA and GB can be also calculated according to those equations described above. Note that the larger the value of PA or GB is, the weaker the acid BH is.

To eliminate the basis-set superposition errors (BSSE), which result from the use of an incomplete basis set, the Boys−Bernardi counterpoise technique has been used.[55]

To explore the solvent effects of aqueous solution on the calculated PAs and GBs in the protonation and deprotonation processes qualitatively, the isodensity surface polarized continuum model (IPCM),[56] which has been successful in the descriptions of several chemical systems in solution,[57−60] has been employed on the basis of the optimized gas-phase geometries.

All the computations were performed at 298.15 K and 1.0 atm using the Gaussian 98 program, and the SCF convergence criteria *Tight* has been used throughout the calculations.[61]

3. Results and Discussions

The calculated relative energies for the protonated and deprotonated glycinamide conformers at various levels of theory are summarized in Tables 1 and 3, respectively. The calculated ZPVE corrections, BSSE corrections, and entropy contributions to the GBs during the protonation and deprotonation processes are presented in Table 2. The corresponding PAs and GBs in the deprotonation processes are summarized in Table 4. The optimized neutral, protonated, and deprotonated glycinamide conformers have been displayed in Figures 1, 2, and 3, respectively. Figure 4 depicts the molecular electrostatic potential energy maps for the four neutral glycinamide conformers. The dependencies of the PA, GB, and the entropy changes on temperature for conformer IB upon amino N3-protonation have been depicted in Figure 5. In the Supporting Information, Table S1 presents the selected structural parameters of the optimized structures for the neutral glycinamide conformers. The calculated relative energies among the neutral glycinamide conformers are also given in Table S2 for reference. Tables S3 and S4 list the selected structural parameters of the optimized structures for the protonated and deprotonated glycinamide conformers, respectively. Tables S5 and S7 summarize the calculated electronic protonation energies in the protonation and deprotonation processes, respectively. Table S6 presents the calculated electronic energy differences between the charged and the neutral forms in aqueous solution employing the IPCM model based on the optimized gas-phase geometries. The corresponding vibrational frequencies and IR intensities for the protonated and deprotonated forms are depicted in Figures S1 and S2, respectively. Temperature dependencies of the calculated PAs, GBs, and entropy contributions to GBs are illustrated in Figures S3−S8, respectively. Additionally, the calculated dipole moments and rotational constants for the neutral, protonated, and deprotonated glycinamide conformers are also presented in Tables S1, S3, and S4, respectively, which should be helpful in the observation or search for these conformers using microwave spectroscopy and rotational spectroscopy experimentally.

TABLE 2: Calculated ZPVE Corrections, BSSE Corrections, and Entropy Contributions to the Calculated GBs during the Protonation and Deprotonation Processes[a,b]

active sites		ΔZPVE	BSSE	$-T\Delta S$
N4[N4]	IB	8.37(8.70)[7.75]	0.47(0.39)[0.68]	−0.30(−0.35)[−1.29]
	IIB	7.75(7.99)[7.28]	0.29(0.47)[0.76]	−1.67(−1.62)[−1.18]
	IIIB	7.88(8.12)[6.74]	0.30(0.50)[0.82]	−0.88(−0.83)[−2.47]
	IV	8.11[8.24]	0.42[0.68]	−0.81[−0.83]
N3[N3]	IB	10.96(10.96)[8.87]	0.77(0.82)[0.74]	−0.16(−0.15)[0.18]
	IIB	10.40(10.41)[9.42]	0.65(0.68)[0.74]	−1.31(−1.32)[1.34]
	IIIB	10.54(10.54)[9.29]	0.58(0.87)[0.74]	−0.53(−0.53)[0.55]
	IV	10.46(10.46)[9.37]	0.75(0.75)[0.74]	−0.59(−0.59)[0.61]
C2[O5]	IB	9.29(9.29)[8.27]	0.55(0.41)[0.20]	−0.54(−0.54)[0.12]
	IIB	8.88(8.88)[8.94]	0.46(0.44)[0.54]	−0.94(−0.94)[1.71]
	IIIB	9.01(9.34)[8.81]	0.39(0.41)[0.54]	−0.15(−0.35)[0.92]
	IV	8.97(8.96)[8.77]	0.52(0.52)[0.20]	−0.84(−0.84)[0.56]
[O5′]	IB	[8.25]	[0.20]	[0.31]
	IIB	[8.36]	[0.21]	[0.62]
	IIIB	[8.42]	[0.20]	[−0.22]
	IV	[8.74]	[0.20]	[0.75]

[a] The data in parentheses and in brackets refer to those of the other hydrogen loss in the deprotonation processes and those of the results in the protonation processes, respectively. [b] All the units are in kcal/mol.

TABLE 3: Relative Energies (in kcal/mol) and ZPVEs (in kcal/mol) for Deprotonated Glycinamide Conformers at Various Levels of Theory[a,b,c]

conformers	B3LYP	ΔZPVE	MP2	MP3	MP4(SDQ)	CCSD(T)
DP1(N4)	0.0(0.0)[0.0]	0.0	0.0	0.0	0.0	0.0
DP2(N4)	9.15(8.83)[1.42]	−0.32	9.56	9.55	9.57	9.46
DP3(N4)	0.09(0.18)[0.19]	0.09	0.14	0.12	0.05	0.01
DP4(N4)	4.80(4.65)[0.58]	−0.15	5.17	5.09	5.12	4.95
DP5(N4)	6.60(6.39)[−0.45]	−0.21	7.17	7.10	7.12	7.00
DP6(N3)	23.69(21.12)[24.53]	−2.57	25.09	26.31	26.15	25.79
DP7(C2)	18.99(18.08)[14.74]	−0.91	21.39	20.73	21.73	21.97
DP8(C2)	17.69(16.65)[15.90]	−1.04	19.57	18.85	19.88	20.06
DP9(C2)	23.43(22.06)[17.59]	−1.37	25.69	24.90	25.88	26.12
DP10(C2)	20.03(18.96)[16.70]	−1.07	22.32	21.79	22.71	22.83

[a] The total energies for DP1(N4) with B3LYP, MP2, MP3, MP4(SDQ), and CCSD(T) are −264.073684, −263.4457662, −263.4582912, −263.4741934, and −263.5085273 hartrees, respectively. The ZPVE for DP1(N4) is 49.25 kcal/mol. [b] The data in parentheses refer to the relative energies with ZPVE corrections. [c] The data in brackets refer to the relative energies in aqueous solution obtained employing the IPCM model within the framework of SCRF theory. The solvation energy of DP1(N4) is −61.96 kcal/mol.

TABLE 4: Calculated Proton Affinities (in kcal/mol) and Gas-Phase Basicities (in kcal/mol) of the Deprotonated Glycinamide Conformers for the Three Active Sites[a]

		N4	N3	C2
IB	PA	358.73(367.63)	379.54(379.50)	376.72(376.87)
	GB	359.02(367.98)	379.70(379.65)	377.27(377.41)
IIB	PA	357.55(361.84)	378.16(378.11)	373.86(373.87)
	GB	359.22(363.46)	379.47(379.43)	374.80(374.82)
IIIB	PA	356.43(360.70)	377.10(376.81)	372.81(378.19)
	GB	357.31(361.53)	377.63(377.34)	372.96(378.54)
IV	PA	362.26	376.67(376.67)	374.73(374.73)
	GB	363.07	377.26(377.26)	375.57(375.57)

[a] The data in parentheses refer to the corresponding PA values of the other hydrogen loss at the same active site.

3.1. Protonation Processes. *3.1.1. Structural Characteristics.* Full geometry optimizations reveal that there are nine stable stationary points on the PES of the protonated glycinamide as displayed in Figure 2, in which one corresponds to N3-protonation, three correspond to N4-protonation, and five correspond to O5-protonation, respectively. Considering the lack of structural information experimentally, it is necessary to analyze the structural changes for neutral glycinamide upon protonation before discussing the PAs and GBs. As mentioned above, there are three active sites, namely, N3, N4, and O5 in neutral glycinamide (see Figure 1). For the carbonyl O5 site, there are two directions of proton attack, that is, the adding proton lies in the cis or trans position with respect to the amide N4 site. As discussed below, protonation occurring at the three sites can result in different structural changes for neutral glycinamide.

For the amino N3-protonation, all the glycinamide conformers are collapsed to the same structure P1(N3) during the course of the geometry optimizations. Like most protonated amino acids,[11] the amino N is the most basic site, which is consistent with the findings of Kinser et al.[8] Actually, the same structure has also been obtained by Kinser et al. employing the MP2/6-31G(d,p) level of theory. Obviously, P1(N3) is characterized by the intramolecular H-bond formed between O5 and H9 as displayed in Figure 2. The strength of its H-bond can be assessed from the following two points: One is the larger bond length for N3−H9 versus N3−H10(H12) (∼1.06 versus 1.02 Å). The other is the smallest stretching vibrational frequency for N3−H9 (∼2877.7 cm^{-1}) relative to the symmetry (asymmetry) vibrational frequency for N3−H10 and N3−H12 (∼3462.9 (∼3520.3) cm^{-1}). More importantly, the vibrational frequency for N3−H9 possesses the strongest IR intensity among all the IR intensities occurring in P1(N3) as displayed in Figure S1 of the Supporting Information, which provides the spectral proof for its identification experimentally. Compared with the most stable protonated glycine, P1(N3) possesses a stronger intramolecular H-bond, which can be confirmed by the shorter H-bond contact distance (∼1.727 Å) relative to that in protonated glycine (∼1.914 Å) obtained at the B3LYP/6-311++G** level of theory. This difference in the strength of the H-bond can be attributed to the fact that the oxygen of an amide is a better H-bond acceptor than the oxygen of a carboxylic acid

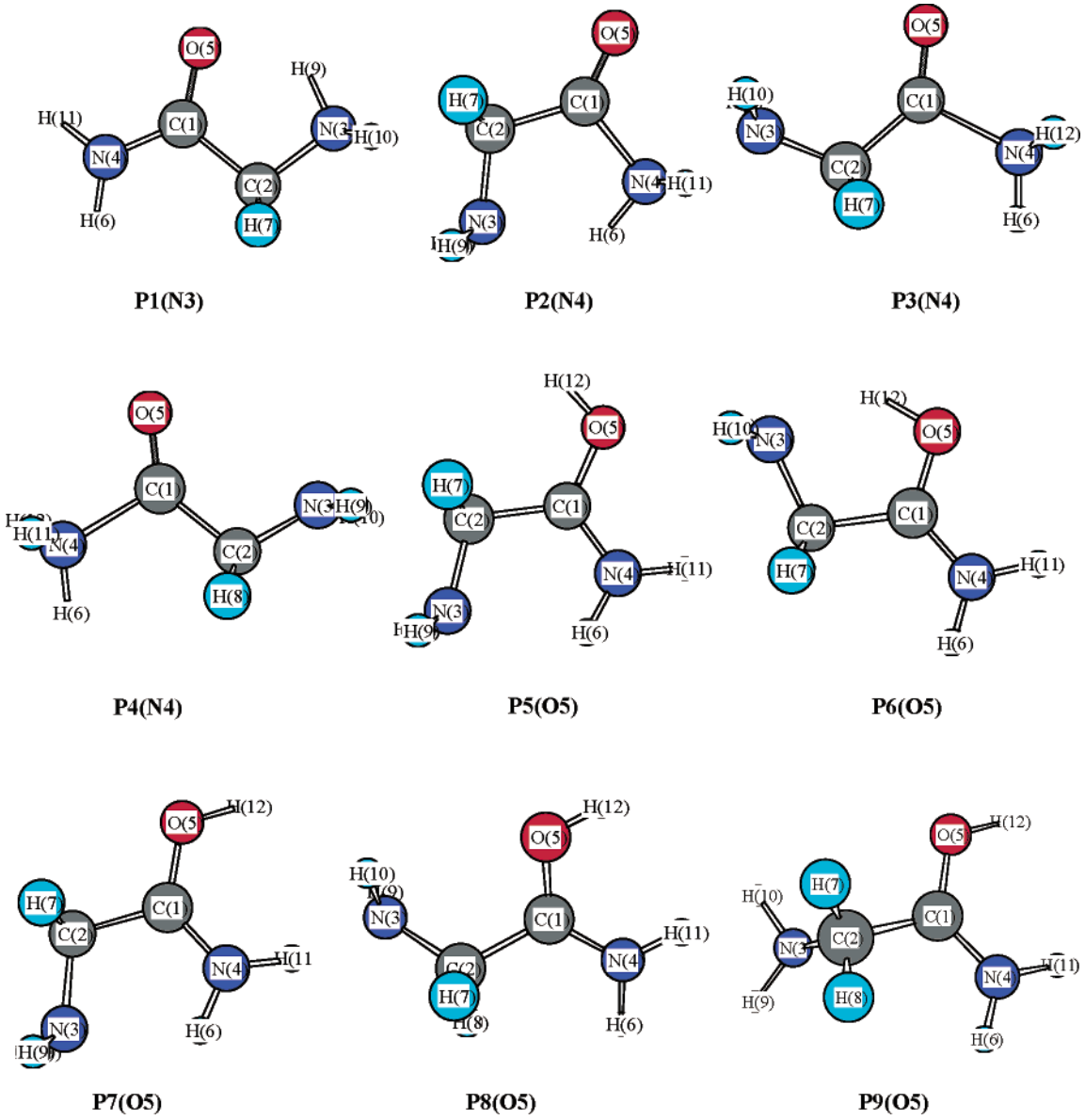

Figure 2. Optimized protonated glycinamide conformers at the B3LYP/6-311++G** level of theory.

group.[8,62,63] It is also worth noting that the neutral glycinamide employed by Kinser et al. in the calculations of PA corresponds to the second most stable glycinamide IIB as displayed in Figure 1. Probably, it is the best approach to test the relative stabilities between IB and IIB using the MP2/6-31G(d,p) level of theory employed by Kinser et al.[8] The computational results show that IIB is 1.098 kcal/mol higher in energy than IB including zero-point vibrational energy (ZPVE) corrections. Of course, it is easy to form P1(N3) via N3-protonation of IIB from a structural point of view. Additionally, both the single-bond of C1═O5 and the double-bond character of the peptide bond (C1−N4) are strengthened, which can be illustrated from the increments in bond length of the C1═O5 (∼0.006 Å) and C1−N4 bond (∼ −0.03 Å) relative to those in the neutral glycinamide conformers. Moreover, the planarity of the peptide bond in P1-(N3) is still kept as those of the neutral glycinamide conformers.[51]

For amide N4-protonation, three optimized geometries have been found, namely, P2(N4), P3(N4), and P4(N4) as displayed in Figure 2. Obviously, P2(N4) is characterized by the intramolecular H-bond formed between N3 and H6, where the H-bond contact distance is 1.93 Å, comparable to the value of 1.89 Å mentioned by Kinser et al.[8] However, another two N4-protonated glycinamide conformers, P3(N4) and P4(N4), had not been reported previously. Compared with neutral glycinamide conformers, both the double-bond of C1═O5 and the single-bond character of the peptide bond (C1−N4) are strengthened strongly, where the increments in bond length are about −0.05 Å and 0.28 Å for the former and the latter, respectively. Obviously, these change trends are completely opposite to those of the N3-protonation process mentioned above.

As far as carbonyl O5-protonation is concerned, the proton can attack the O5 atom in two directions as mentioned above. For the two trans O5-protonated conformers, namely, P5(O5) and P6(O5), both of them are characterized by the intramolecular H-bonds, where the H-bond contact distances are 2.142 and 1.741 Å for the former (N3···H6) and the latter (N3···H12), respectively. The shorter intramolecular H-bond distance in P6-(O5) indicates that it is more stable than P5(O5) as further confirmed by the comparisons of the total energies between them below. From a structural point of view, P7(O5) can be obtained via changing the proton (H12) position in P5(O5). Moreover, the strength of the intramolecular H-bond in P7(O5) is larger with respect to P5(O5) since the H-bond contact distance is

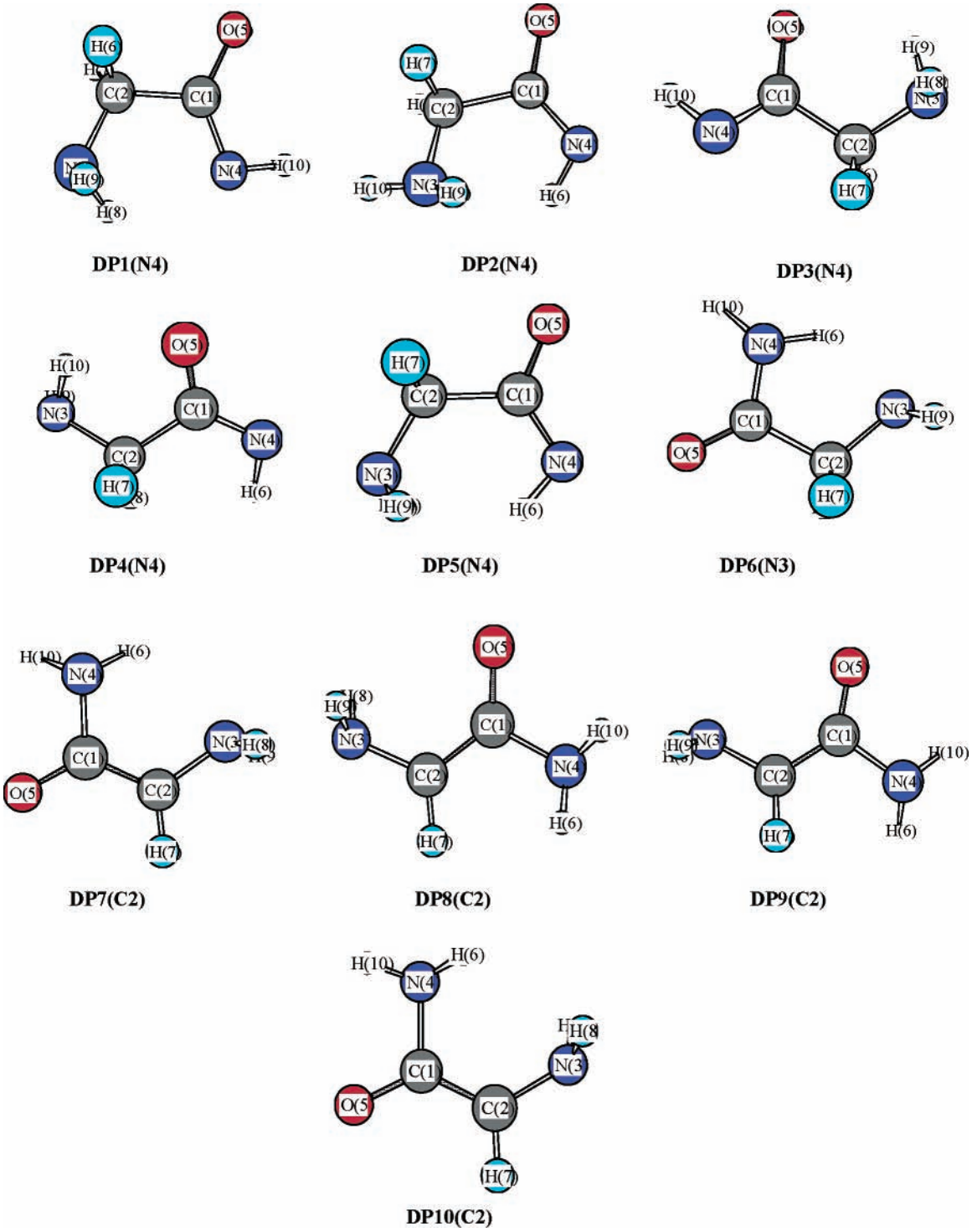

Figure 3. Optimized deprotonated glycinamide conformers at the B3LYP/6-311++G** level of theory.

2.075 Å versus 2.142 Å. Compared with the results of Kinser et al.,[8] only P7(O5) had been mentioned for O5-protonation. In fact, P5(O5) and P7(O5) can be easily obtained through the O5-protonation of neutral glycinamide conformer IB from a structural point of view. Similarly, both P8(O5) and P9(O5) can be obtained via the O5-protonation of glycinamide IIB and IIIB, respectively, where the plane of N3C2C1 for the latter is almost perpendicular to that of O5C1C2(~82.31°). Compared with the water molecule, all the bond lengths of O5−H12 in the O5-protonated forms except for P6(O5) are larger by about 0.01 Å than that of water (~0.96 Å). Correspondingly, their stretching frequencies (from 3721.6 to 3753 cm^{-1}) are smaller than those of water, where the symmetric and asymmetric stretching vibrational frequencies of O−H in H_2O are 3816.7 and 3921.9 cm^{-1} obtained at the B3LYP/6-311++G** level of theory, respectively. In P6(O5), the bond length of O5−H12 is about 0.06 Å larger than that of water and its vibrational frequency is 2900.4 cm^{-1} with the strongest IR intensity as shown in Figure S1 of the Supporting Information. The smallest stretching vibrational frequency and longest bond length of O5−H12 in P6(O5) among the O5-protonated forms should be attributed to the formation of the strong intramolecular H-bond as mentioned above. Like the amino N3-protonation, both the single-bond of C1═O5 and the double-bond character of the peptide bond (C1−N4) are strengthened upon O5-protonation, which can be illustrated from the increments in bond length of

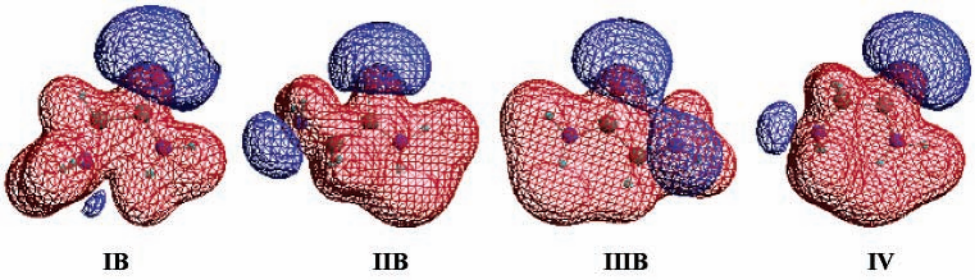

Figure 4. Molecular electrostatic potential energy maps for the four neutral glycinamide conformers.

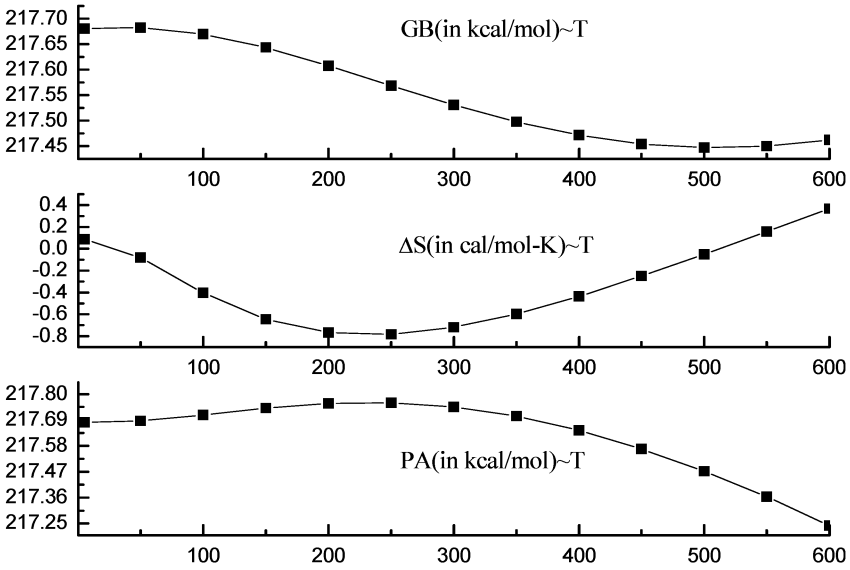

Figure 5. Dependencies of PA, GB, and the entropy changes on temperature at 1.0 atm for conformer IB upon amino N3-protonation.

the C1═O5 (∼ +0.08Å) and C1−N4 bonds (∼ −0.06 Å) relative to those in neutral glycinamide conformers. What is more, the planarity of the peptide bond in all the O5-protonated glycinamide conformers is still kept as those of the neutral and N3-protonated forms.

3.1.2. Relative Stabilities. Table 1 presents the calculated relative energies for the protonated glycinamide conformers at various levels of theory. Overall, the relative stabilities for the different protonation sites are as follows: N3 > O5 > N4, where N3-protonation stabilizes the whole system by more than 10.0 and 25.1 kcal/mol relative to the average values for O5- and N4-protonation, respectively. Moreover, the relative stabilities described above have been well reproduced by higher-level calculations employing MP2, MP3, MP4(SDQ), and CCSD(T) levels on the basis of the optimized geometries using the B3LYP/6-311++G** level of theory. Thus, the unique N3-protonation product P1(N3) should be the global minimum among the available protonated forms, where the intramolecular H-bond formed between O5 and H9 should play an important role in stabilizing the whole molecule.

For the three N4-protonated forms, P3(N4) and P4(N4) are 7.66 and 8.34 kcal/mol higher in energy than P2(N4), which may be attributed to the existence of the intramolecular H-bond formed between N3 and H6 in P2(N4).

For the O5-protonated forms, the relative stabilities among them are as follows: P8(O5) < P9(O5) < P7(O5) < P5(O5) < P6(O5), where the energy separations relative to P6(O5) fall in the range from 4.42 to ∼15.31 kcal/mol. Similarly, the stability of P6(O5) may be derived from the intramolecular H-bond formed between N3 and H12. For example, the intramolecular H-bond contact distance in P6(O5) is obviously shorter than those in P5(O5) and P7(O5) (1.74 Å versus 2.14 and 2.08 Å). P7(O5) is 1.41 kcal/mol higher in energy than P5(O5) despite the fact that the strength of the N3···H6−N4 intramolecular H-bond in P7(O5) with a shorter N3···H6 bond length is slightly larger than that in P5(O5). Actually, in both cases (P7(O5) and P5(O5)) the N3···H6−N4 H-bonds are basically equivalent, and the stability of P5(O5) over P7(O5) should be attributed to the existence of another H−bond, O5···H11, originating from the interaction of H11 with the lone-pair electrons of O5 in P5-(O5). This may be proved by the smaller bond angle ∠N4C1O5 (118.4°) in P5(O5) than that (125.9°) in P7(O5). Obviously, although the slightly stronger N3···H6−N4 H-bond in P7(O5) than that in P5(O5) makes a more positive contribution to the stability of P7(O5), both the H11···O5 H-bond in P5(O5) and the H11···H12 repulsion interaction in P7(O5) make more positive contributions to the stability of P5(O5) relative to P7-(O5), and the overall effect of the three factors results in P5-(O5) being more stable than P7(O5). Similarly, another two cis-position O5-protonated forms, that is, P8(O5) and P9(O5), are much higher in energy than those trans-position forms (P5(O5) and P6(O5)).

Additionally, as presented in Table 1, the ZPVE corrections cannot change the relative stabilities among the available protonated glycinamide conformers. Obviously, the ZPVE corrections tend to stabilize other conformers relative to P1-(N3). In other words, the energy separations relative to P1(N3) become small for other conformers since the ZPVE of P1(N3) is the largest among the protonated glycinamide conformers followed by the O5- and N4-protonated forms.

The relative stabilities among the three different active sites have been reported by Kinser et al.,[8] that is, the resulting isomer

2 (P1(N3) in the present paper) is 10.28 kcal/mol more stable than the O-protonated form 3 (P7(O5) in the present paper) calculated at the MP2/6-31G(d,p) level, which in turn is 9.08 kcal/mol more stable than isomer 4 (P2(N4) in the present paper) protonated at the amide nitrogen. These above predictions are well reproduced by our present calculations, where P1(N3) is 7.86 kcal/mol more stable than P7(O5), and P7(O5) is 11.90 kcal/mol more stable than P2(N4) including ZPVE corrections.

To explore the solvent effect on the relative stabilities among the available protonated glycinamide conformers, the IPCM model within the framework of self-consistent reaction field (SCRF) theory has been employed on the basis of the optimized gas-phase geometries at the B3LYP/6-311++G** level of theory. As presented in Table 1, the solvent does not modify the above relative stabilities in the gas phase except between P8(O5) and P9(O5). P1(N3) is still the most stable conformer in aqueous solution followed by the second stable conformer P6(O5) at 11.81 kcal/mol. The reverse order between P8(O5) and P9(O5) may be derived from the larger difference in dipole moments associated with the solvation energy directly, where the dipole moment and solvation energy is 5.40 versus 3.44 D and −69.07 versus −67.50 kcal/mol for the former and the latter, respectively.

3.1.3. PA and GB Calculations. It is reported that protonation of the neutral molecule can be analyzed from the molecular electrostatic potential (MEP), which has proven to be useful in rationalizing interaction between molecules and in molecular recognition process.[10] Qualitatively, Figure 4 displays the MEPs of the four neutral glycinamide conformers on the basis of the optimized gas-phase geometries employing the B3LYP/6-311++G** level of theory. As can be seen from Figure 4, the electronegative zones created by the oxygen atom are further extended in space and deeper than those created by the amino nitrogen atom. Especially, in the regions around amide nitrogen atom, there are not any signs indicating that the proton can be attached. Thus, it seems that the oxygen atom should be the favorable protonation site over the other two nitrogen atoms. For the MEP of conformer IB, the minor probability of the proton attack on the amino nitrogen atom should be due to the formation of the intramolecular H-bond between the amide and the amino group. Actually, all three active sites can be attacked by the proton according to our calculations employing the B3LYP/6-311++G** level of theory. The discrepancies between MEPs and actual calculations may be due to the fact that the former are predicted on the assumption that the interaction is purely electrostatic.[9] Furthermore, the MEP is a static reactivity index and it changes in the process.[10]

Table S5 of the Supporting Information presents the calculated electronic protonation energies, which are defined as the negative values of the energy differences between the protonated and neutral forms. Note that the relative order of magnitude of the PAs and GBs for the three active sites[51] are well reproduced by the electronic protonation energies using the B3LYP/6-311++G** level of theory and higher-level calculations. Thus, the preferred site for protonation should be N3 followed by O5 and N4. Moreover, for the O5-protonation, the trans arrangement of the proton is more favorable relative to that of the cis arrangement. Considering the experimental uncertainties, the calculated PA (216.81 kcal/mol) for the most stable glycinamide is in good agreement with the experimental value (217.73 kcal/mol).[8] Thus, neutral glycinamide should behave as an amino N3-base in the gas phase. Compared with glycine, the PA of glycinamide is larger than that of glycine (from 202.8 to 215.7 kcal/mol),[3,5,11,12] which is consistent with the report of Kinser et al.[8] As expected, the reason can be attributed to the stabilizing effect of the amide group in glycinamide relative to the carboxylic acid group in glycine, and the protonated glycinamide (P1(N3)) possesses a stronger intramolecular H-bond than that of glycine as mentioned above.

As listed in Table 2, the BSSEs produced in the calculations of the PAs and GBs are calculated to be not more than 0.9 kcal/mol, a relatively small quantity, implying that the 6-311++G** adopted here should be an appropriate basis set. Comparisons of the BSSEs and ZPVE corrections indicate that the latter are more important for the calculations of PAs and GBs.

As also can be seen from Table 2, the different entropy contributions to the Gibbs free energies can be used to understand the smaller GBs relative to the corresponding PAs except for the N4-protonation. Obviously, all the $T\Delta S$ values are very small, indicating that ΔG is essentially determined by ΔH. As expected, the negative value of the enthalpy indicates that the protonation process is an exothermic reaction.

Additionally, the solvent and temperature effects on the protonation processes have been investigated as a preliminary and tentative study. As displayed in Figures S3 and S4 of the Supporting Information, the PAs and GBs for the three active sites exhibit different trends versus temperature. These different changes should be related to the entropy changes as displayed in Figure S5 of the Supporting Information. For example, for the N3-protonation of IB, the PA increases gently until it reaches a maximum around 250 K, and then it decreases gradually with increasing temperature as displayed in Figure 5. On the other hand, the GB decreases gently until it reaches a minimum around 500 K, and then it increases slightly when the temperature rises. The above different change trends can be elucidated by the entropy changes versus temperature. Namely, as displayed in Figure 5, the entropy changes should play a key role relative to PA though PA increases gently before 250 K, resulting in the decreasing of GB. In the ranges from 250 to ∼500 K, the PA should predominate over the role of entropy though entropy increases monotonically, still resulting in the decreasing of GB. At around 500 K, the GB is controlled almost entirely by the PA since the entropy approaches zero. When the temperature exceeds 500 K, once again the entropy plays a key role relative to PA. Thus, the GB begins to increase when the temperature rises.

To explore the solvent effect of an aqueous solution on the protonation processes qualitatively, only the electronic energy differences between the charged and neutral species have been considered throughout the following studies since the solvation energy of the proton has the same effect on every protonation process. As listed in Table 1, in aqueous solution the protonated glycinamide conformers are much better stabilized by solvation than those of the neutral forms, where the solvation energies are about −68 kcal/mol versus −11 kcal/mol for the former and the latter, respectively. As displayed in Table S6 of the Supporting Information, comparisons of the energy differences between the protonated and unprotonated forms in aqueous solution indicate that glycinamide still behaves as an amino N3-base. Compared with the results in the gas phase, the strength of the N3-base is clearly larger than those of the N4- and O5-bases. Of course, these treatments in aqueous solution here do not represent the realistic situation for glycinamide. More extensive theoretical investigations on the protonation and deprotonation processes in solution are in progress in our laboratory.

3.2. Deprotonation Processes. *3.2.1. Structural Characteristics.* For the deprotonation processes, all the possibilities of

the loss of a proton have been considered for the six hydrogen atoms attached to the amide N4, amino N3, and C2 atom, respectively. As a result, 10 structures have been located on the PES of the deprotonated glycinamide conformers as displayed in Figure 3.

For the deprotonation of amide N4, five conformers have been found, that is, from DP1(N4) to DP5(N4). Obviously, all of them are characterized by the formation of intramolecular H-bonds with the exception of DP5(N4) though the strength of the H-bonds may be weaker than those of the protonated forms if only the H-bond contact distance is considered, where the H-bond distance is 2.28, 2.31, 2.25, and 2.19 Å for the N4···H8 in DP1(N4), N3···H6 in DP2(N4), O5···H9 in DP3(N4), and O5···H10 in DP4(N4), respectively. Compared with those neutral glycinamide conformers, both the single-bond of C1═O5 and the double-bond character of the peptide bond (C1−N4) are strengthened upon N4-deprotonation. Furthermore, these phenomena have been reproduced by the N3-deprotonation processes, in which only one conformer has been found, that is, DP6(N3) characterized by the intramolecular H-bond formed between N3 and H6 (about 1.77 Å). However, those changes for the C1−N4 (C1−O5) bond upon N3- and N4-deprotonation are clearly different, where the increments of the bond lengths are −0.04 (+0.05) and −0.02 (+0.03) Å for the former and the latter, respectively. In the case of C2-deprotonation, four conformers have been found as displayed in Figure 3 from DP7-(C2) to DP10(C2). Obviously, the planarity of the peptide bond in neutral glycinamide has been destroyed upon C2-deprotonation. For example, the dihedral angles of O5−C1−N4−H10 are −34.77°, 30.15°, −27.70°, and −23.62° for DP7(C2), DP8-(C2), DP9(C2), and DP10(C2), respectively. Additionally, the strengths of the peptide bond C1−N4 and the C1═O5 bond are weakened relative to those in the neutral forms, where the increments are about +0.1 and +0.05 Å, respectively.

Compared with glycine, the global minimum DP1(N4) has a similar structure to that of the most stable deprotonated glycine.[7] However, the deprotonated glycine possesses a slightly stronger intramolecular H-bond formed between one of the hydrogen atoms at the amino nitrogen site and the carbonyl oxygen relative to that of DP1(N4), where the intramolecular H-bond contact distances are 2.22 and 2.28 Å for the former and the latter obtained at the B3LYP/6-311++G** level of theory, respectively.

3.2.2. Relative Stabilities. Table 3 gives the calculated relative energies among the available deprotonated forms relative to DP1(N4) along with their corresponding ZPVEs obtained at the B3LYP/6-311++G** level of theory. For the deprotonated conformers, the relative stabilities upon certain site deprotonations have been determined at the B3LYP/6-311++G** level of theory, that is, N4 > C2 > N3, which has been further supported by the higher-level calculations employing MP2, MP3, MP4(SDQ), and CCSD(T) levels. Comparisons of the energy difference between DP1(N4) and DP3(N4) (∼0.18 kcal/mol) suggest that both of them should be essentially equal in energy though higher-level calculations favor of the stability of DP1(N4) slightly. On the other hand, the relative stabilities between DP6(N3) and DP9(C2) may change with and without ZPVE corrections at the B3LYP/6-311++G** level of theory, indicating the importance of the ZPVE corrections again. Moreover, the ZPVE corrections tend to stabilize the N3-deprotonated conformer followed by the C2-deprotonated forms relative to those N4-deprotonated forms since the ZPVEs for N4-deprotonation are the largest among the available conformers followed by those for C2- and N3-deprotonation, respectively. In fact, the ZPVE-corrected relative stabilities between DP6-(N3) and DP9(C2) are reproduced by the MP2 and CCSD(T) calculations. Considering the favorable ZPVE corrections for DP6(N3), it is more probable that DP6(N3) is slightly more stable than DP9(C2) at the MP3 and MP4(SDQ) levels if considering ZPVE corrections. Certainly, much higher-level calculations are required to further verify the relative stabilities between them.

As displayed in Table 3, in aqueous solution, the relative stabilities among the available deprotonated glycinamide conformers have been changed by solution. Namely, the most stable conformer is not DP1(N4) but DP5(N4), and DP7(C2) is 1.16 kcal/mol more stable than DP8(C2) due to the solvent effect, where the solvation energies for DP1(N4), DP5(N4), DP7(C2), and DP8(C2) are −61.96, −69.01, −66.21, and −63.75 kcal/mol, respectively. These phenomena are consistent with the relative order of magnitude in dipole moments among them since the larger dipole moments should result in an extra stabilization in aqueous solution, where the larger dipole moments for DP5-(N4) (5.7 D) and DP7(C2) (4.62 D) are favorable over DP1-(N4) (2.52 D) and DP8(C2) (2.0 D) in the gas phase.

3.2.3. PAs and GBs. Table S7 of the Supporting Information and Table 4 present the calculated electronic protonation energies, PAs, and GBs in the deprotonation processes. Like the protonation processes, the electronic protonation energies for the three different sites, that is, N4, N3, and C2, are consistent with the calculated PAs and GBs for the deprotonated glycinamide conformers. Thus, it is a good way to predict the acidity or basicity for the different active sites qualitatively employing the calculated electronic protonation energy.

As listed in Table 4, comparisons of the PAs and GBs for the three different sites indicate that the PAs (GBs) at the N3 and C2 sites are about 17.09 (16.81) and 14.49 (14.21) kcal/mol larger than those at the N4 site. The differences in PAs or GBs for the removal of the different protons at the same site are larger for N4 (∼5.8 kcal/mol) followed by C2 (∼1.4 kcal/mol) and N3 (∼0.1 kcal/mol), indicating the nonequivalence of the two H atoms at the same active site except for those in C_s symmetry conformer IV. As mentioned above, for the deprotonation processes, the larger the PA is, the weaker the acidity is. Thus, glycinamide should behave as an N4−H acid, and the N3−H acidity is predicted to be nearly the same as that of C2−H in the gas phase.

Once again, the ZPVE corrections are much larger than the BSSEs as listed in Table 2, indicating that ZPVE corrections should be considered whether in the protonation or deprotonation processes. At the same time, all the entropies in the deprotonation processes should play the same role since they have the same order of magnitude, which can be further illustrated from the fact that all the GBs are larger than their corresponding PAs as listed in Table 4. Additionally, like those in the protonation processes, the dependencies of the PAs, GBs, and entropy changes on the temperature depicted in Figures S6−S8 of the Supporting Information in the deprotonation processes should be helpful in understanding the acid−base behavior of glycinamide at different temperatures.

As listed in Table S6 of the Supporting Information, in aqueous solution, glycinamide still behaves as an N4−H acid as supported by the fact that the electronic energy differences between the deprotonated and their corresponding neutral forms are the smallest for N4-deprotonation followed by those for the C2- and N3-deprotonation.

As expected, comparisons with the acidity of glycine ranging from 340.3 to 342.0 kcal/mol[7,13] indicate that the acidic strength

of glycine is larger than that of glycinamide, which may be due to the stabilizing effect of the amide group in glycinamide relative to the carboxylic acid group in glycine, and the deprotonated glycinamide possesses a weaker intramolecular H-bond than that of glycine as mentioned above.

4. Conclusions

In the present study, a systematic study about the protonation and deprotonation of glycinamide has been performed considering all the different active sites employing the B3LYP/6-311++G** level of theory. A total of 9 (10) representative protonated (deprotonated) glycinamide conformers have been found. The structural characteristics for these conformers have been discussed. Both the global minima for the protonated and deprotonated glycinamide conformers are characterized by the formation of intramolecular H-bonds. The relative stabilities among the available protonated and deprotonated glycinamide conformers have been determined correctly at the B3LYP/6-311++G** level of theory, which are further confirmed by the higher-level calculations, including MP2, MP3, MP4(SDQ), and CCSD(T) levels. Comparisons of the calculated electronic protonation energies, PAs, and GBs at different active sites indicate that glycinamide should behave as an amino N3-base and amide N4−H acid in the gas phase. Similarly, in aqueous solution, glycinamide is also predicted to behave as an amino N3-base and amide N4−H acid employing the IPCM model within the framework of SCRF theory. Moreover, the temperature effects have been investigated qualitatively for the protonation and deprotonation processes. For future studies on systems related to glycinamide, a conclusion should be drawn that B3LYP performs quite well and should be used as a relatively inexpensive and reliable approach for the investigation of the acid−base behavior of larger biological systems.

Acknowledgment. This work is supported by the National Natural Science Foundation of China (Grant 20273040) and the Natural Science Foundation of Shandong Province (Key project); support from SRFDP and the Foundation for University Key Teacher by the Ministry of Education is also acknowledged. We are also grateful to the referees for their insightful suggestions to improve the presentation of the results.

Supporting Information Available: Table S1 presents the selected structural parameters of the optimized structures for the neutral glycinamide conformers; the calculated relative energies among the neutral glycinamide conformers are also given in Table S2 for reference; Tables S3 and S4 list the selected structural parameters of the optimized structures for the protonated and deprotonated glycinamide conformers, respectively; Tables S5 and S7 summarize the calculated electronic protonation energies in the protonation and deprotonation processes, respectively; Table S6 presents the calculated electronic energy differences between the charged and the neutral forms in aqueous solution employing the IPCM model based on the optimized gas-phase geometries; the corresponding vibrational frequencies and IR intensities for the protonated and deprotonated forms are depicted in Figures S1 and S2, respectively; temperature dependencies of the calculated PAs, GBs, and entropy contributions to GBs are illustrated in Figures S3−S8, respectively. This material is available free of charge via the Internet at http://pubs.acs.org.

References and Notes

(1) Vayner, E.; Ball, D. W. *J. Mol. Struct. (THEOCHEM)* **2000**, *496*, 175.
(2) Kovačević, B.; Glasovac, Z.; Maksić, Z. B. *J. Phys. Org. Chem.* **2002**, *15*, 765.
(3) Topol, I. A.; Burt, S. K.; Toscano, M.; Russo, N. *J. Mol. Struct. (THEOCHEM)* **1998**, *430*, 41.
(4) Cassady, C. J.; Carr, S. R.; Zhang, K.; Chung-Phillips, A. *J. Org. Chem.* **1995**, *60*, 1704.
(5) Zhang, K.; Chung-Phillips, A. *J. Phys. Chem. A* **1998**, *102*, 3625.
(6) Harrison, A. G. *Mass Spectrom. Rev.* **1997**, *16*, 201.
(7) Topol, I. A.; Burt, S. K.; Russo, N.; Toscano, M. *J. Am. Soc. Mass Spectrom.* **1999**, *10*, 318.
(8) Kinser, R. D.; Ridge, D. P.; Hvistendahl, G.; Rasmussen, B.; Uggerud, E. *Chem.—Eur. J.* **1996**, *2*, 1143.
(9) Russo, N.; Toscano, M.; Grand, A.; Jolibois, F. *J. Comput. Chem.* **1998**, *19*, 989.
(10) Muñoz-Caro, C.; Niño, A.; Senent, M. L.; Leal, J. M.; Ibeas, S. *J. Org. Chem.* **2000**, *65*, 405.
(11) Maksić, Z. B.; Kovačević, B. *Chem. Phys. Lett.* **1999**, *307*, 497.
(12) Noguera, M.; Rodríguez-Santiago, L.; Sodupe, M.; Bertran, J. *J. Mol. Struct. (THEOCHEM)* **2001**, *537*, 307.
(13) Locke, M. J.; McIver, R. T., Jr. *J. Am. Chem. Soc.* **1983**, *105*, 4226.
(14) Jensen, F. *J. Am. Chem. Soc.* **1992**, *114*, 9533.
(15) Bliznyuk, A. A.; Schaefer, H. F., III; Amster, I. J. *J. Am. Chem. Soc.* **1993**, *115*, 5149.
(16) Ventura, O. N.; Rama, J. B.; Turi, L.; Dannenberg, J. J. *J. Am. Chem. Soc.* **1993**, *115*, 5754.
(17) Lin, H.; Ridge, D. P.; Uggerud, E.; Vulpius, T. *J. Am. Chem. Soc.* **1994**, *116*, 2996.
(18) Bouchoux, G.; Defaye, D.; McMahon, T.; Likholyot, A.; Mó, O.; Yáñez, M. *Chem.—Eur. J.* **2002**, *8*, 2900.
(19) Del Bene, J. E.; Shavitt, I. *J. Phys. Chem.* **1990**, *94*, 5514.
(20) Del Bene, J. E. *J. Phys. Chem.* **1993**, *97*, 107.
(21) Hillebrand, C.; Klessinger, M.; Eckert-Maksić, M.; Maksić, Z. B. *J. Phys. Chem.* **1996**, *100*, 9698.
(22) Merrill, G. N.; Kass, S. R. *J. Phys. Chem.* **1996**, *100*, 17465.
(23) Peterson, K. A.; Xantheas, S. S.; Dixon, D. A.; Dunning, T. H., Jr. *J. Phys. Chem. A* **1998**, *102*, 2449.
(24) Wang, F.; Ma, S.; Zhang, D.; Cooks, R. G. *J. Phys. Chem. A* **1998**, *102*, 2988.
(25) Roy, R. K.; De Proft, F.; Geerlings, P. *J. Phys. Chem. A* **1998**, *102*, 7035.
(26) González, A. I.; Mó, O.; Yáñez, M. *J. Phys. Chem. A* **1999**, *103*, 1662.
(27) Chandra, A. K.; Nguyen, M. T.; Uchimaru, T.; Zeegers-Huyskens, T. *J. Phys. Chem. A* **1999**, *103*, 8853.
(28) Russo, N.; Toscano, M.; Grand, A.; Mineva, T. *J. Phys. Chem. A* **2000**, *104*, 4017.
(29) Podolyan, Y.; Gorb, L.; Leszczynski, J. *J. Phys. Chem. A* **2000**, *104*, 7346.
(30) Bouchoux, G.; Choret, N.; Berruyer-Penaud, F. *J. Phys. Chem. A* **2001**, *105*, 3989.
(31) Remko, M. *J. Phys. Chem. A* **2002**, *106*, 5005.
(32) Lee, H.-J.; Choi, Y.-S.; Lee, K.-B.; Park, J.; Yoon, C.-J. *J. Phys. Chem. A* **2002**, *106*, 7010.
(33) Gomes, J. R. B.; Ribeiro da Silva, M. A. V. *J. Phys. Chem. A* **2003**, *107*, 869.
(34) (a) Zhang, K.; Chung-Phillips, A. *J. Chem. Inf. Comput. Sci.* **1999**, *39*, 382. (b) Zhang, K.; Chung-Phillips, A. *J. Comput. Chem.* **1998**, *19*, 1862.
(35) Kovačević, B.; Maksić, Z. B. *Org. Lett.* **2001**, *3*, 1523.
(36) Senent, M. L.; Niño, A.; Muñoz-Caro, C.; Ibeas, S.; García, B.; Leal, J. M.; Secco, F.; Venturini, M. *J. Org. Chem.* **2003**, *68*, 6535.
(37) Wolken, J. K.; Tureček, F. *J. Am. Soc. Mass Spectrom.* **2000**, *11*, 1065.
(38) Smets, J.; Houben, L.; Schoone, K.; Maes, G.; Adamowicz, L. *Chem. Phys. Lett.* **1996**, *262*, 789.
(39) Rogalewicz, F.; Hoppilliard, Y. *Int. J. Mass Spectrom.* **2000**, *199*, 235.
(40) Bourcier, S.; Hoppilliard, Y. *Int. J. Mass Spectrom.* **2002**, *217*, 231.
(41) Deakyne, C. A. *Int. J. Mass Spectrom.* **2003**, *227*, 601.
(42) Uggerud, E. *Theor. Chem. Acc.* **1997**, *97*, 313.
(43) Jursic, B. S. *J. Mol. Struct. (THEOCHEM)* **1999**, *487*, 193.
(44) Oie, T.; Loew, G. H.; Burt, S. K.; MacElroy, R. D. *J. Am. Chem. Soc.* **1984**, *106*, 8007.
(45) Jensen, J. H.; Baldridge, K. K.; Gordon, M. S. *J. Phys. Chem.* **1992**, *96*, 8340.

(46) Remko, M.; Rode, B. M. *Chem. Phys. Lett.* **2000**, *316*, 489.
(47) Remko, M.; Rode, B. M. *Phys. Chem. Chem. Phys.* **2001**, *3*, 4667.
(48) Klassen, J. S.; Kebarle, P. *J. Am. Chem. Soc.* **1997**, *119*, 6552.
(49) Sulzbach, H. M.; Schleyer, P. V. R.; Schaefer, H. F., III. *J. Am. Chem. Soc.* **1994**, *116*, 3967.
(50) Ramek, M.; Cheng, V. K. W. *Int. J. Quantum Chem., Quantum Biol. Symp.* **1992**, *19*, 15.
(51) Li, P.; Bu, Y.; Ai, H. *J. Phys. Chem. A* **2003**, *107*, 6419.
(52) Li, P.; Bu, Y.; Ai, H. *J. Phys. Chem. B* **2004**, *108*, 1405.
(53) Li, P.; Bu, Y.; Ai, H. *J. Phys. Chem. A* **2004**, *108*, 1200.
(54) Johnson, B. G.; Gill, P. M. W.; Pople, J. A. *J. Chem. Phys*. **1993**, *98*, 5612.
(55) Boys, S. F.; Bernardi, F. *Mol. Phys.* **1970**, *19*, 553.
(56) Foresman, J. B.; Keith, T. A.; Wiberg, K. B.; Snoonian, J.; Frisch, M. J. *J. Phys. Chem.* **1996**, *100*, 16098.
(57) Li, X.; Sevilla, M. D.; Sanche, L. *J. Am. Chem. Soc.* **2003**, *125*, 8916.
(58) Li, X.; Sanche, L.; Sevilla, M. D. *J. Phys. Chem. A* **2002**, *106*, 11248.
(59) Lee, I.; Kim, C. K.; Han, I. S.; Lee, H. W.; Kim, W. K.; Kim, Y. B. *J. Phys. Chem. B* **1999**, *103*, 7302.
(60) Kovacevic, B.; Maksic, Z. B. *Org. Lett.* **2001**, *3*, 1523.
(61) Frisch, M. J.; Trucks, G. W.; Schlegel, H. B.; Scuseria, G. E.; Robb, M. A.; Cheeseman, J. R.; Zakrzewski, V. G.; Montgomery, J. A., Jr.; Stratmann, R. E.; Burant, J. C.; Dapprich, S.; Millam, J. M.; Daniels, A. D.; Kudin, K. N.; Strain, M. C.; Farkas, O.; Tomasi, J.; Barone, V.; Cossi, M.; Cammi, R.; Mennucci, B.; Pomelli, C.; Adamo, C.; Clifford, S.; Ochterski, J.; Petersson, G. A.; Ayala, P. Y.; Cui, Q.; Morokuma, K.; Malick, D. K.; Rabuck, A. D.; Raghavachari, K.; Foresman, J. B.; Cioslowski, J.; Ortiz, J. V.; Stefanov, B. B.; Liu, G.; Liashenko, A.; Piskorz, P.; Komaromi, I.; Gomperts, R.; Martin, R. L.; Fox, D. J.; Keith, T.; Al-Laham, M. A.; Peng, C. Y.; Nanayakkara, A.; Gonzalez, C.; Challacombe, M.; Gill, P. M. W.; Johnson, B. G.; Chen, W.; Wong, M. W.; Andres, J. L.; Head-Gordon, M.; Replogle, E. S.; Pople, J. A. *Gaussian 98*, revision A.9; Gaussian, Inc.: Pittsburgh, PA, 1998.
(62) Taylor, R.; Kennard, O.; Versichel, W. *Acta Crystallogr., Sect. B* **1984**, *40*, 280.
(63) Meot-Ner, M. *J. Am. Chem. Soc.* **1984**, *106*, 1257.